

## ATOMIC AND MOLECULAR CARBON AS A TRACER OF TRANSLUCENT CLOUDS

ERIC B. BURGH, KEVIN FRANCE

Center for Astrophysics and Space Astronomy, University of Colorado - Boulder, 593 UCB, Boulder, CO 80309

AND

EDWARD B. JENKINS

Princeton University Observatory, Peyton Hall, Ivy Lane, Princeton, NJ 08544.

*Draft version July 1, 2018*

## ABSTRACT

Using archival, high-resolution far-ultraviolet *HST*/STIS spectra of 34 Galactic O and B stars, we measure C I column densities and compare them with measurements from the literature of CO and H<sub>2</sub> with regard to understanding the presence of translucent clouds along the line-of-sight. We find that the CO/H<sub>2</sub> and CO/C I ratios provide good discriminators for the presence of translucent material, and both increase as a function of molecular fraction,  $f^N = 2N(\text{H}_2)/N(\text{H})$ . We suggest that sightlines with values below CO/H<sub>2</sub>  $\approx 10^{-6}$  and CO/C I  $\approx 1$  contain mostly diffuse molecular clouds, while those with values above sample clouds in the transition region between diffuse and dark. These discriminating values are also consistent with the change in slope of the CO v. H<sub>2</sub> correlation near the column density at which CO shielding becomes important, as evidenced by the change in photochemistry regime studied by Sheffer et al. (2008). Based on the lack of correlation of the presence of translucent material with traditional measures of extinction we recommend defining 'translucent clouds' based on the molecular content rather than line-of-sight extinction properties.

*Subject headings:* ISM: abundances, ISM: clouds, ISM: lines and bands, ISM: molecules

## 1. INTRODUCTION

In the traditional three phase interstellar medium (ISM), the cold neutral medium (CNM) contains the bulk of the interstellar "clouds". These clouds range from the dense dark clouds, the centers of which are the birthplaces of the next generation of stars, typically observed by CO radio emission, to the tenuous diffuse clouds, which can be probed by absorption spectroscopy of background stars.

In the literature, these are typically defined by their extinction properties, with the diffuse ISM having  $A_V \lesssim 1$  and the dense clouds having  $A_V \gtrsim 5$  (van Dishoeck & Black 1988). This distinction by extinction indicates the importance of the ultraviolet portion of the interstellar radiation field on the photochemistry in the clouds. The diffuse ISM is fully exposed, and therefore most species exist in atomic or ionized forms. In dense clouds the ultraviolet light is sufficiently shielded such that molecules are not photodissociated and virtually all the hydrogen exists in molecular form (H<sub>2</sub>), with carbon monoxide (CO) the second most abundant molecule.

Sightlines with intermediate extinction tend to be referred to as "translucent". A translucent sightline may simply be the concatenation of multiple diffuse clouds, resulting in a higher value of  $A_V$  than is typical of a sightline that might pass through a single diffuse cloud. One may also sample the transition region between the diffuse and dense clouds, where species make the transition between their atomic and molecular forms – what could be considered a translucent "cloud". In these regions the chemistry is sensitive to the physical conditions, such as density, temperature and radiation field, which may be changing rapidly from one location to the next. With increased depth into a cloud comes

an increased fraction of molecular content, both in H<sub>2</sub> because of self-shielding, and CO, because of shielding by H<sub>2</sub>, as well as the attenuation of photodissociating flux by dust (van Dishoeck & Black 1988). In the case of hydrogen, the transition from atomic to molecular form is quite sharp, with the local molecular fraction ( $f^n = 2n(\text{H}_2)/n_{\text{H}}$ ,  $n \equiv$  space density) reaching essentially a value of one at very short depths into a cloud. Observations of the integrated molecular fraction ( $f^N = 2N(\text{H}_2)/N(\text{H})$ ,  $N \equiv$  column density) show a sharp jump from values less than  $\sim 10^{-4}$  to values larger than  $\sim 0.01$  consistent with the presence of this transition (Spitzer & Jenkins 1975; Gillmon et al. 2006), and as a consequence H<sub>2</sub> is ubiquitous in the diffuse ISM (Shull et al. 2000). The gas-phase carbon makes a transition from ionized form (C II) to molecular (CO). Although the calculated depth at which this transition happens and the relative abundances of all the carbon-bearing species depends on the physical parameters and chemical networks used, this qualitative description appears in all models (Röllig et al. 2007).

The far-ultraviolet (far-UV:  $\lambda \lesssim 2000\text{\AA}$ ) portion of the electromagnetic spectrum allows for the direct observation of both H<sub>2</sub> and CO in the ISM through absorption spectroscopy towards distant O and B stars (Savage et al. 1977; Rachford et al. 2002; Federman et al. 1980; Burgh et al. 2007; Sheffer et al. 2008). In particular, the study of Rachford et al. (2002) investigates the molecular content and physical properties along lines-of-sight considered translucent by their extinction properties, reaching the conclusion that they are likely the projections of multiple diffuse clouds with low extinction rather than a single translucent cloud with higher extinction. Burgh et al. (2007) suggested that the ratio of CO to H<sub>2</sub> would serve as a better discriminator of

diffuse and translucent clouds and they measure a transition from low to high values of  $\text{CO}/\text{H}_2$  with increased molecular fraction. The CO abundance is more sensitive to the effects of geometry, dust shielding and fragmentation of clouds, and thus if a given sightline were simply a collection of diffuse clouds, there would not be an increase in the measured  $\text{CO}/\text{H}_2$  (Kopp et al. 2000). If the term “translucent” should refer to the transition region between the physical states of “diffuse” and “dense” then these results demonstrate a weakness in defining translucent clouds based solely on line-of-sight extinction or  $\text{H}_2$  properties.

Snow & McCall (2006) recommend a different definition for “translucent”, based upon the carbon content, specifically the transition from ionized to molecular form. This suggests that observations of neutral carbon (C I), also available in the far-UV (Jenkins & Shaya 1979; Jenkins & Tripp 2001), may give further insight as to the presence of translucent clouds along a given sightline. Steady-state PDR models predict that C I is formed through recombination of C II and photodissociation of CO, and its abundance should peak in the region between the ionic and molecular parts of the cloud. Snow & McCall (2006) then further break down cloud structure into the following categories (see their Table 1): diffuse atomic, where the low molecular fractions mentioned earlier are observed; diffuse molecular, where the hydrogen is primarily molecular, but carbon still in ionized form; translucent, where the carbon makes the transition to molecular; and dense, where both the hydrogen and carbon are fully molecular. We agree with this type of categorization, eschewing the use of extinction as the sole discriminator.

In this work, we expand upon the study of Burgh et al. (2007) by including measurements of the C I lines observed in the *HST*/STIS E140H mode. We compare these measurements to CO and  $\text{H}_2$  in an attempt to better isolate the transition from diffuse to translucent and better understand the conditions under which this transition occurs.

## 2. COLUMN DENSITY DETERMINATIONS

### 2.1. $\text{H}_2$ and CO

This work expands on the data set used in Burgh et al. (2007), by adding sightlines with  $\text{H}_2$  column density determinations by Sheffer et al. (2008), Nehmé et al. (2008), Rachford et al. (2009), and Shull et al. (2009). CO column density determinations are from Burgh et al. (2007), Sheffer et al. (2008), as well as six new fits, determined in the same manner as in Burgh et al. (2007). Although a larger dataset exists with both  $\text{H}_2$  and CO column densities, we are presenting here only those for which there existed adequate wavelength coverage of STIS E140H data for the C I measurement, described in the next section.

The total number of sightlines is 34 and range from diffuse to translucent material, with extinctions from  $E(B-V) = 0.07 - 0.61$ ,  $\text{Log } N(\text{H}_2) = 18.73 - 20.92$ , with molecular fractions ranging from 0.02 - 0.76. The CO column densities have some upper limits around 12.3 but mostly detections in the range  $\text{Log } N(\text{CO}) = 12.98 - 16.13$ . Table 1 lists the column densities for the hydrogen bearing species and Table 2 lists those for carbon, both with ap-

propriate references.

### 2.2. H I

For the most part, the H I column densities are taken from the literature and determined from profile fits of the Ly- $\alpha$  line (Diplas & Savage 1994; Fitzpatrick & Massa 1990; Rachford et al. 2002; Cartledge et al. 2004; Jensen et al. 2007). However, in a few cases, the spectral type of the star is late enough such that contamination from the stellar Ly- $\alpha$  prevents an accurate determination of the interstellar atomic hydrogen column density. For three cases (HD 27778, HD 147888, and HD 203532), we use the Bohlin et al. (1978) relationship between  $N(\text{H}_{\text{tot}})$  and  $E(B - V)$  to determine the total hydrogen column density.

HD 102065, however, poses an interesting problem. Burgh et al. (2007) state that the presence of weak C IV absorption features seemed to indicate that the original spectral type identification of B9IV was wrong and reclassified the star as a B2V, an early enough type to allow for Ly- $\alpha$  profile fitting. However, the analysis of Nehmé et al. (2008) suggests that the C IV could be from hot interstellar gas along the line-of-sight, and thus the original identification may be correct. For this study, we will assume that is true and determine the H I column from the Bohlin relationship. This is not an insignificant issue because the difference in molecular fraction between the two cases is large ( $f^N = 0.10$  if B2V and  $f^N = 0.69$  if B9IV). This will be commented upon later in the results section.

### 2.3. C I

The C I column densities were determined following the method of Jenkins & Tripp (2001), which takes advantage of a large number of multiplets including a wide range in line strengths to provide solutions for the apparent column densities  $N_a$  as a function of radial velocity. This is done for each of the C I, C I\*, and C I\*\* levels. The column density for each level is obtained by integrating over the full velocity range<sup>1</sup> and then the total column density, presented in Table 2, is the sum of each level. The Jenkins & Tripp (2001) method is not conducive to determining a random error for the velocity integrated column density, so we adopt an error of 0.05 dex, or  $\sim 12\%$ , which is consistent with similar determinations from other methods.

The  $N_a$  profiles were determined using two values of the “transition intensity” mentioned in Equation (7) in Section 5.2.1 of Jenkins & Tripp (2001). This parameter reduces the weight on the parts of the lines that are strongly saturated in the original data. In 31 of the 34 cases, the lower ( $I_t = 0.2$ ) and higher ( $I_t = 0.4$ ) values produced column densities with differences less than 0.05 dex. Furthermore, for the sightlines that will be defined as “diffuse” by the criteria mentioned later, the maximum difference is 0.02 dex, which is within our

<sup>1</sup> It is of interest to note that some sightlines show velocity components with more column in the excited states than the ground states, indicative of higher thermal pressure. However, these are typically seen at higher velocities, thus unrelated to the clouds in which the molecules reside, and also amount to a small fraction of the total column. We have made no effort to isolate any specific velocity range for integration in order to exclude these regions.

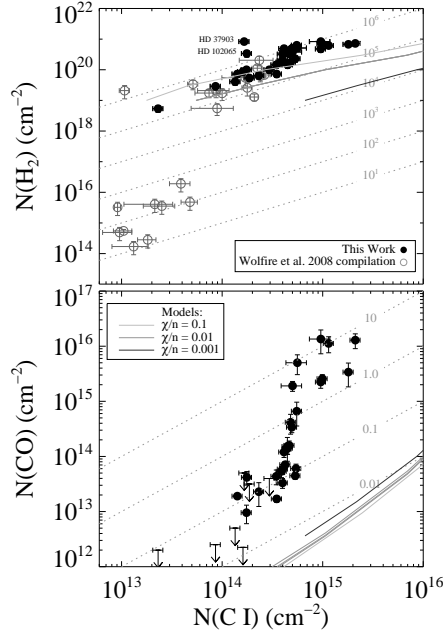


**Figure 1.**  $\text{H}_2$  and CO versus C I. Arrows designate upper limits on the CO measurement. Dashed lines show the ratio of the each species with C I. Overplotted are models from Visser et al. (2009) for varying values of the ratio of the strength of the interstellar radiation field to the density ( $\chi/n$ ).

adopted minimum error in  $N(\text{C I})$ . In the three remaining cases the differences were: 0.1 dex (HD 24534), 0.16 dex (HD 147888), and 0.24 dex (HD 203532). This indicates that in these cases, there is likely to be unresolved saturated velocity structure affecting the result, and we assign a larger error (0.10 dex) to these. To err on the side of being conservative, we have used the higher value of  $I_t$  for all cases because it is likely to produce a more accurate result for those sightlines that suffer from unresolved saturated velocity structure and makes little difference for those that do not.

It is important to note here that we are using the oscillator strengths from Jenkins & Tripp (2001), which differ from those of theoretical and experimental derivations compiled in Morton (2003). This can result in large differences in derived column density; e.g., Sonnentrucker et al. (2002) and Sonnentrucker et al. (2003) derive total C I column densities of  $\text{Log } N(\text{C I})=15.37$  and  $\text{Log } N(\text{C I})=15.57$  for HD 192639 and HD 185418, respectively. These differ by factors of about 4 and 7 from the values determined in this study. The differences in oscillator strengths grow systematically with a decrease in strength, as shown in Figure 3 of Jenkins & Tripp (2001), so the greater the column density the larger the deviation because more weight will be placed on the weaker lines in the derivation. We believe that given the self-consistency in the results provided by the rederived  $f$ -values we are justified in using them. Furthermore, the trends found in our study should be unaffected by these kinds of systematic changes in column density, except for potential slope changes in correlations because of the strength dependence of the deviations.

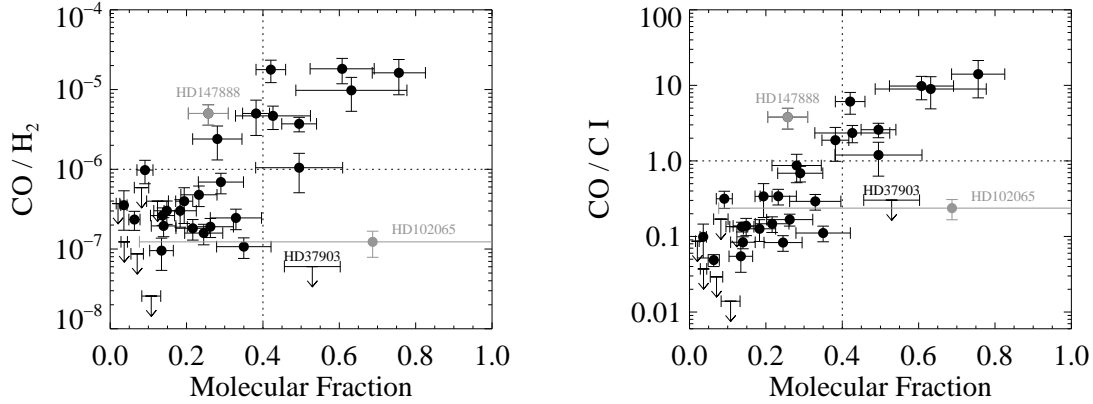
### 3. RESULTS

Figure 1 shows the relationships between  $\text{H}_2$ , CO and C I. Included in the upper panel are C I values from the literature and compiled in Wolfire et al. (2008) to give a broader context to the data presented here. The lack of sightlines with  $\text{H}_2$  column densities in the range of about  $10^{17}$  to  $10^{18}$  represents the turn-on of  $\text{H}_2$  due to self-shielding (Gillmon et al. 2006), as evidenced by the fact that the low  $\text{H}_2$  column sightlines all have a  $f^N \lesssim 10^{-4}$  and the sightlines in our sample all have  $f^N > 0.01$ . In the lower panel, the CO/C I shows a trend with a steep slope,  $N(\text{CO}) \propto N(\text{C I})^{2.5}$ , with the CO column density rising over two orders of magnitude for a small range in C I. There may be a hint of a slope change similar to that found in the CO versus  $\text{H}_2$  relationship near  $N(\text{CO})$  of  $10^{14}$  (Sheffer et al. 2008). At about  $\text{Log } N=14.7$  there is as much CO as C I along the line-of-sight, and the trend suggests the observation of the transition from diffuse to translucent molecular material, where CO becomes the dominant carbon-bearing species.

The CO/C I is similar to CO/ $\text{H}_2$  in its utility as a discriminator between the diffuse and translucent regimes. Figure 2 shows both ratios versus molecular fraction. As discussed by Burgh et al. (2007), the CO/ $\text{H}_2$  shows a transition from low to high between  $f^N = 0.2$  and  $f^N = 0.4$ . CO/C I shows a stronger correlation ( $r \sim 0.8$ , excluding the outliers) with values above 1 for  $f^N > 0.4$ .

There are a few notable exceptions to the relationships observed in Figure 2: HD 147888, HD 37903, and HD 102065. HD 147888 ( $\rho$  Oph D) lies in a complex area of the sky, deeply investigated by Snow et al. (2008). There is no direct H I column density determination, so it is possible that the molecular fraction is underestimated. In terms of molecular content it appears more like a translucent sightline than other sightlines of similar  $f^N$ . As mentioned in Section 2.2, the  $f^N$  for HD 102065 depends strongly on the spectral type classification of the star, which might be in doubt because of observed C IV absorptions, which may or may not be of stellar origin. The molecular content is consistent with a diffuse cloud, as would be expected if the lower  $f^N$  were correct, and Nehmé et al. (2008) do find a best model fit for low density ( $n \sim 80 \text{ cm}^{-3}$ ). The HD 37903 sightline is unique in our sample for having its  $\text{H}_2$  in very close proximity to the star, such that there are observed absorptions out of vibrationally excited levels. Meyer et al. (2001) show that this is consistent with a dense parcel of gas being illuminated by a flux about 1000 times the strength of the average ultraviolet interstellar radiation field. This intense flux would be strong enough to photodissociate the CO in that cloud, and thus, even though the molecular fraction is about 0.5, there is at best only a marginal detection of CO. It would make for an interesting comparison to explore, with a rejuvenated STIS, other nebular environments, such as the sightlines to HD 34078, which also shows absorption from highly excited  $\text{H}_2$  (Boissé et al. 2005), and HD 200775, where *IUE* data show a very high CO column density (Knauth et al. 2001).

Figure 3 shows, for a sub-sample of 21 sightlines with  $A_V$  determined by Valencic et al. (2004), scatter plots of  $f^N$ , CO/ $\text{H}_2$  and CO/C I against  $A_V$ . No significant correlations or trends are seen, indicating that line-of-sight extinction is not a good measure of the molecular content in the transition between diffuse and translucent



**Figure 2.** CO/H<sub>2</sub> (left) and CO/C I (right) versus molecular fraction. The CO/H<sub>2</sub> transitions from low (diffuse) to high (translucent) between  $f^N=0.2-0.4$ , with all values above  $10^{-6}$  by  $f^N=0.4$ . The CO/C I shows a linear relationship with  $f^N$ , with all values above 1 by  $f^N=0.4$ . HD102065 (the  $f^N$  error for which is quite large due to uncertainties in the spectral classification), HD147888 and HD37903 are notable exceptions and are discussed in the text.

clouds. In particular, one should note that some of the largest CO column densities are seen for sightlines with  $A_V \lesssim 1$ . Translucent cloud models are overplotted and will be discussed in Section 4.4.

#### 4. DISCUSSION

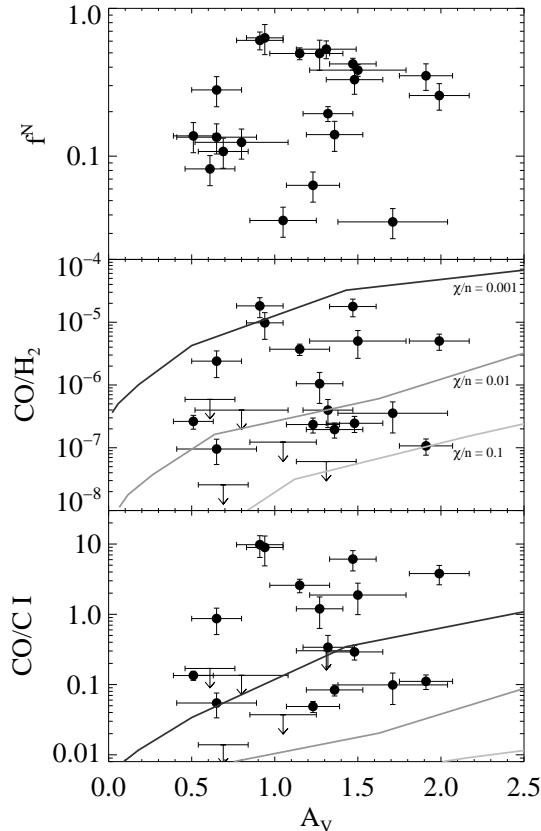


**Figure 3.** Molecular fraction, CO/H<sub>2</sub> and CO/C I versus  $A_V$ , for a sub-sample of 21 stars with  $A_V$  determined by Valencic et al. (2004). Overplotted are models from Visser et al. (2009) for varying values of the ratio of the strength of the interstellar radiation field to the density ( $\chi/n$ ). These show that translucent clouds could be present along sightlines with low  $A_V$  if  $\chi/n$  is also low.

#### 4.1. Diffuse to Translucent Transition

The measured quantities along a given sightline are, by nature, integrated quantities and may not be indicative of the local values of the material through which the line-of-sight passes. Historically, the word “translucent” has been applied to sightlines of a given  $A_V$ ; however, following Snow & McCall (2006) we believe the distinction between diffuse and translucent should be made based on the local values of the material sampled. Therefore, we use the words diffuse and translucent to describe sightlines based on the type of cloud sampled (i.e., low or high local neutral carbon content), independently of the line-of-sight extinction.

Based on the correlations seen in Figure 2 we believe we are seeing the transition from diffuse to translucent clouds being probed for sightlines with  $f^N \gtrsim 0.4$ . More specifically we suggest the values of CO/H<sub>2</sub> =  $10^{-6}$  and CO/C I = 1 as discriminating values between sightlines with diffuse and translucent clouds. Those sightlines with measurements above these values are almost completely inclusive of each other, independently of molecular fraction. This is shown explicitly in Figure 4. Although we expect C I to peak in the translucent cloud regime, it is primarily the steep increase in CO abundance that is driving the observations. The standouts from Figure 2 are well-behaved in Figure 4, indicating that these ratios are more reliable than molecular fraction alone in distinguishing between sightlines with diffuse and translucent clouds; e.g., regardless of the uncertainty in the H I determinations for HD 102065 and HD 147888, these sightlines clearly have diffuse and translucent material, respectively.

This is supported by the work of Sheffer et al. (2008), who recently analyzed a large sample of Galactic sightlines with far-UV data of CO and H<sub>2</sub>, in addition to optical data of other carbon-bearing molecules. They conclude that at higher column densities there is a distinct change from low- to high-density photochemistry. They delineate the change at Log N(CO)=14.1 and Log N(H<sub>2</sub>)=20.4, the point at which the CO vs. H<sub>2</sub> correlation changes slope. Above Log N=20.4 in H<sub>2</sub> there is still a wide range in CO/H<sub>2</sub> and CO/C I, most likely

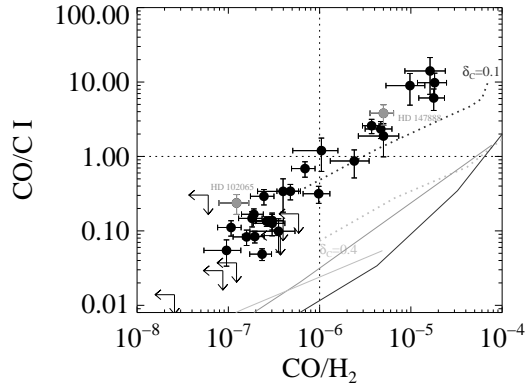


**Figure 4.** CO/C I versus CO/H<sub>2</sub>. Arrows designate upper limits on the CO measurement. We will identify those sightlines with CO/H<sub>2</sub>  $\gtrsim 10^{-6}$  and CO/C I  $\gtrsim 1$  as “translucent”. The solid lines are models from Visser et al. (2009) with colors following those in the previous figures. The dashed lines are translucent cloud models from van Dishoeck & Black (1988) with two different values of carbon depletion.

due to sightline to sightline variations in the ratio of the strength of the radiation field to the density ( $\chi/n$  hereafter) and/or cloud structure/fragmentation. Above Log  $N=14.1$  of CO we find some sightlines with total neutral content (see discussion below) that look diffuse. If we make a cut based on the total neutral carbon content we find that Log  $N(\text{CO})=14.6$  is a better value for discriminating the two regimes and is fully consistent with the values we suggested above of CO/H<sub>2</sub> =  $10^{-6}$  and CO/C I = 1.

#### 4.2. Single versus Multiple Clouds

In the range of  $A_V$  sampled in this study, extinction properties give no indication of the physical or chemical conditions in the clouds sampled along the line-of-sight; therefore, a sightline with a given  $A_V$  may sample a thick cloud with translucent material, or simply be overlapping clouds with more diffuse material.

This is an important distinction to make, as evidenced by the studies of translucent sightlines by Rachford et al. (2002, 2009). They came to the conclusion that their lines of sight sample multiple diffuse clouds rather than truly “translucent” clouds; however, we note that 31/38 have  $f^N > 0.2$  and about half have  $f^N > 0.4$ . This suggests that, despite their expectations for high extinction and  $f^N = 1$ , it is likely that a large fraction of their sightlines do include clouds with significant molecular content. Indeed, they admit that were they to relax their requirement for large  $A_V$  they would conclude that ten of their lines-of-sight contain translucent clouds. These ten, which include HD 24534 and HD 27778 (two of our highest CO/H<sub>2</sub> values), were noted specifically for having larger  $f^N$  and lower H<sub>2</sub> rotational temperatures.

Mathematically speaking,  $f^N$  is an average value for the sightline, which must sample some material with  $f^n > f^N$ . The presence of a translucent cloud, where  $f^n \approx 1$ , could be somewhat hidden by an extensive foreground of diffuse atomic material, where  $f^n$  is likely to be less than  $10^{-4}$ . Browning et al. (2003) claim that, based on their H<sub>2</sub> properties alone, they were unable to model these sightlines as a single cloud of high extinction, but

instead they were more successful with concatenations of smaller clouds of lower extinction each; i.e., there must be multiple pathways for radiation getting in. However, this is in contradiction with the high abundance of CO, as shown in the CO/H<sub>2</sub> and CO/C I relationships.

We note that two of the stars in that sample, HD 192639 and HD 185418, were studied in detail by Sonnentrucker et al. (2002) and Sonnentrucker et al. (2003), respectively. In both cases, they came to the conclusion that translucent material was not seen, which would seem to bolster the Rachford et al. claim. However, these prove to be good examples in our current study: HD 192639, for example, has a high  $A_V$  (1.91) and reasonably high molecular fraction ( $f^N = 0.35$ ), but has both a low CO/H<sub>2</sub> ( $1.07 \times 10^{-7}$ ) and CO/C I (0.11). Both of these values are consistent with a diffuse cloud. HD 185418 is a borderline case (CO/H<sub>2</sub> =  $1.05 \times 10^{-6}$  and CO/C I = 1.25).

According to models of individual clouds, the transition from atomic to molecular hydrogen, dominated by self-shielding, happens very quickly, over a short range of extinction. Therefore, the transition from C II to CO is occurring in a region where  $f^n \approx 1$ , regardless of the value of  $f^N$ . Outside of the diffuse molecular clouds,  $f^N$  is typically  $< 10^{-4}$  and probably consistent with  $f^n$ . Thus, for  $f^N \gtrsim 0.01$ , the value of  $f^N$  is indicative of the amount of hydrogen along the line of sight that has  $f^n \approx 1$  and the trends shown in Figure 2 put a constraint on the fragmented structure of the diffuse ISM. With increasing molecular fraction, we observe an increasing CO content such that the high  $f^N$  sightlines cannot be too porous, letting in CO-photodissociating far-UV radiation, but must include significant amounts of translucent material.

#### 4.3. Neutral Carbon Fraction

It is possible to put the more unusual standouts with respect to molecular fraction in context by looking at the overall neutral fraction of the carbon – the total neutral carbon content per hydrogen nucleon, (C I + CO)/H. This is shown as a function of molecular fraction in Figure 5. Plotted with our results are data from the literature as compiled by Wolfire et al. (2008) to demonstrate the full run over the widest range, including sightlines sampling what is most likely primarily “diffuse atomic” material. These additional points have no CO measurements; however, we use only those sightlines for which  $N(\text{C I}) < 14.0$ , where we expect the CO contribution to be negligible. The gap centered around  $f^N = 10^{-3}$  separates the atomic from the molecular clouds (Spitzer & Jenkins 1975; Gillmon et al. 2006).

In this representation it is clear how the diffuse and translucent sightlines differ. Also, it shows how the diffuse sightlines in our sample have a consistent ionization state with those primarily atomic sightlines, with very small molecular fraction, suggesting that the C I observed along these sightlines most likely exists in the diffuse atomic material, where the C I abundance will be governed by a balance between photoionization and recombination. Those sightlines with higher molecular fraction but lower neutral carbon abundance (such as HD 102065) may indeed, as suggested by Rachford et al. (2002), be a concatenation of diffuse clouds or be sam-

pling material with higher ratios of radiation intensity to density.

The overall fraction of carbon that is in neutral form rises sharply in the translucent regime. Figure 6 shows this as a function of  $\text{CO}/\text{H}_2$ , plotting the value  $(\text{C I} + \text{CO})/\text{H} \div (\text{C}/\text{H})_{\text{cosmic}} \times \delta_{\text{C}}$ . We use the Holweger (2001) solar abundance value (391 ppm) for the cosmic carbon abundance and leave the depletion factor as a free parameter. The dashed line is a fit to the rise for values of  $\text{CO}/\text{H}_2$  greater than  $10^{-6}$ , i.e., the translucent cloud regime, and produces a power law slope of essentially unity:  $\text{Log}_{10}(\text{C}_{\text{neutral}}/\text{C}_{\text{total}}) \propto \text{Log}_{10}(\text{CO}/\text{H}_2)^{1.08 \pm 0.23}$ . For a constant depletion factor, the values in the plot will shift up with the slope unchanged, e.g., if  $\delta_{\text{C}} = 0.1$  then our most translucent sightlines reach nearly 17% neutral fraction for the integrated column densities. However, if there is more depletion in translucent clouds than in the diffuse ISM, the slope may be increased.

#### 4.4. Comparison to Translucent Cloud Models

Because we only measure integrated/averaged quantities we need to make comparisons to models of the ISM in order to get an understanding of what the local values are along a line-of-sight. Figures 1, 4 and 6 show models from the recent work of Visser et al. (2009), who revisited the translucent cloud models of van Dishoeck & Black (1988), using updated values of oscillator strengths, expanding the range of column densities (which include the suprathermal chemistry regime suggested by Sheffer et al. (2008)), and modeling more isotopologues of CO. In particular, we show the curves for three values of the ratio of the strength of the interstellar radiation field ( $\chi$  in units of the Draine (1978) field) to the gas density ( $n$ ). These models do a good job at matching observations of  $\text{H}_2$  and CO (see Visser's

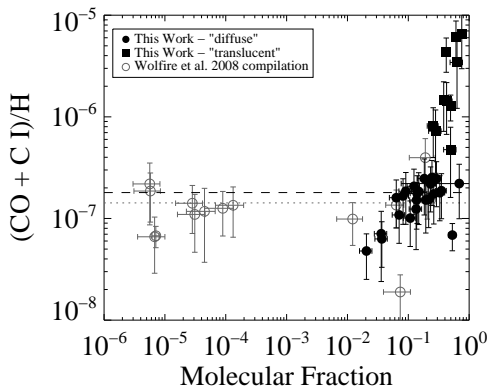


**Figure 5.** Neutral carbon content ( $\text{C I} + \text{CO}$ ) per hydrogen nucleus as a function of molecular fraction. Filled squares and circles are for those sightlines sampling translucent and diffuse material respectively, while open circles represent the sample from Wolfire et al. (2008) for  $\text{Log } N(\text{C I}) < 14.0$  – for these, we expect the CO contribution to be negligible. Dashed and dotted lines are the average values for the diffuse sightlines from this work and the Wolfire compilation respectively, excluding the outliers with  $(\text{C I} + \text{CO})/\text{H} < 8 \times 10^{-8}$ , which are mostly from sightlines that pass through lower density material and/or higher than average radiation environments, such as HD 37903, mentioned previously. HD 93222 and HD 93843 reside near the Carina nebula, while HD 121968 is a halo star, lying behind the Radio Loop I and IV SNRs (Sembach et al. 1997). The lowest neutral fraction is towards HD 143018 ( $\pi$  Sco).

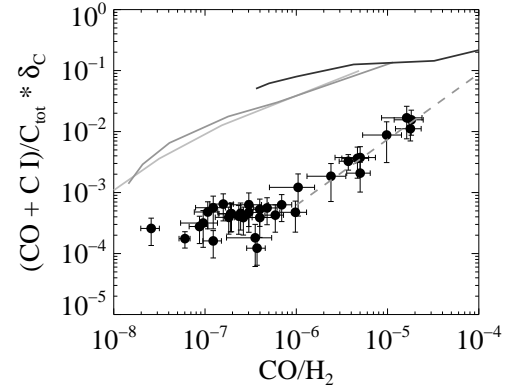


**Figure 6.** Fraction of gas-phase carbon in neutral form multiplied by the depletion factor  $\delta_{\text{C}}$  as a function of  $\text{CO}/\text{H}_2$ . The red line is a fit to the linear rise in the translucent regime ( $\text{CO}/\text{H}_2 > 10^{-6}$ ). Solid lines are models from Visser et al. (2009) with colors following those in the previous figures.

Figure 7); however, we are finding a large discrepancy between the models and the data for C I.

There is even poorer agreement with the data for the models from Röllig et al. (2007), which are specifically for warm and dense photo-dissociation regions and we believe are not well matched to the physical properties in the diffuse and translucent ISM at large. The lowest densities and interstellar radiation field strengths modeled in that work are  $1000 \text{ cm}^{-3}$  and 10 times the Draine (1978) field, respectively, which are at the highest values in the Visser et al. (2009) work.

In Figure 4 we also overplot the cloud models of van Dishoeck & Black (1988), which included two values of the carbon depletion,  $\delta_{\text{C}}$ . The model with the higher value of depletion ( $\delta_{\text{C}} = 0.1$ ) shows a better agreement with the data than does the one with their preferred value ( $\delta_{\text{C}} = 0.4$ ), which is consistent with observational determinations of carbon depletion (Sofia et al. 2004).

This discrepancy may be the result of multiple effects: systematic errors in the oscillator strengths (e.g., use of the Morton (2003) values for the C I lines would produce a larger column densities); inappropriate parameter space in the models, the results of which are sensitive to densities, strengths of the interstellar radiation field, grain models, chemical networks, etc.; or inaccuracies in the carbon depletion determinations – a recent study of the damping wings of the strong C II  $\lambda 1335$  absorption line shows a lower gas phase abundance than determinations from the weaker intersystem lines (Sofia & Parvathi 2008).

We note that Visser et al. (2009) adopted the chemical network of Röllig et al. (2007), which includes only species from the four most abundant elements (H, He, O and C). Röllig et al. (2007) mentions that this network excludes some species that could be important in the chemical balance of carbon in photodissociation regions, such as sulfur. Furthermore, the chemical reactions governing the C I abundance are complicated by the presence of neutral and ionized polycyclic aromatic hydrocarbons (Bakes & Tielens 1998; Wolfire et al. 2008), which can affect the position of the C I abundance peak as a function of depth into a cloud.

Given that the models agree well with  $\text{CO v H}_2$ , we

can comment on their ability to reproduce the CO/H<sub>2</sub> as a function of  $A_V$  (see middle panel of Figure 4). The models show that the primary driver of CO/H<sub>2</sub> is  $\chi/n$ , regardless of the extinction. Our data span two orders of magnitude change in  $\chi/n$ , with the highest CO columns appearing where the  $\chi/n$  is lowest. For a given value of  $A_V$ , geometric effects can greatly change what the measured line-of-sight properties might be (see Figure 4 of Kopp et al. 2000, for example) and thus extinction alone is not a good discriminator of the presence of translucent material.

## 5. CONCLUSIONS

Based upon the results reported here, we suggest that the definition of “translucent” based on measures of extinction be replaced with one based on molecular content, primarily CO. In the range of  $A_V$  sampled in this study, extinction properties give no indication of the physical or chemical conditions in the clouds sampled along the line of sight. We believe this to result primarily from the facts that extinction correlates better with total hydrogen rather than molecular hydrogen and that the penetration of ultraviolet radiation is very sensitive to cloud structure (Kopp et al. 2000).

These observations provide good constraints for models of the interstellar medium. Significant column densities of CO, and high values of CO/H<sub>2</sub>, even at relatively low extinction, suggest that the interstellar medium cannot be too fragmented and porous; i.e., translucent material that is sufficiently shielded from photodissociating far-UV radiation exists in increasing abundance along sightlines with high molecular fraction. These sightlines cannot simply be concatenations of multiple diffuse clouds.

Finally, we point out that, like CO/H<sub>2</sub>, CO/C I can be a good measure of the presence of translucent material along a given line-of-sight. Although the Cosmic Origins Spectrograph aboard the *Hubble Space Telescope* has some ability to measure H<sub>2</sub> along some sightlines (McCandliss et al. 2009), both it and the Space Telescope Imaging Spectrograph are optimized for performance in the 1150–1550 Å range, where CO and C I both have many absorption features and may be measured simultaneously.

We would like to thank R. Visser for providing us with his model results. Some/all of the data presented in this paper were obtained from the Multimission Archive at the Space Telescope Science Institute (MAST). STScI is operated by the Association of Universities for Research in Astronomy, Inc., under NASA contract NAS5-26555. Support for MAST for non-HST data is provided by the NASA Office of Space Science via grant NAG5-7584 and by other grants and contracts.

## REFERENCES

- Bohlin, R. C., Savage, B. D., & Drake, J. F. 1978, *ApJ*, 224, 132
- Boissé, P., Le Petit, F., Rollinde, E., Roueff, E., Pineau des Forêts, G., Andersson, B.-G., Gry, C., & Felenbok, P. 2005, *A&A*, 429, 509
- Browning, M. K., Tumlinson, J., & Shull, J. M. 2003, *ApJ*, 582, 810
- Burgh, E. B., France, K., & McCandliss, S. R. 2007, *ApJ*, 658, 446
- Cartledge, S. I. B., Lauroesch, J. T., Meyer, D. M., & Sofia, U. J. 2004, *ApJ*, 613, 1037
- Diplas, A., & Savage, B. D. 1994, *ApJS*, 93, 211
- Draine, B. T. 1978, *ApJS*, 36, 595
- Federman, S. R., Glassgold, A. E., Jenkins, E. B., & Shaya, E. J. 1980, *ApJ*, 242, 545
- Fitzpatrick, E. L., & Massa, D. 1990, *ApJS*, 72, 163
- Gillmon, K., Shull, J. M., Tumlinson, J., & Danforth, C. 2006, *ApJ*, 636, 891
- Gry, C., Boulanger, F., Nehmé, C., Pineau des Forêts, G., Habart, E., & Falgarone, E. 2002, *A&A*, 391, 675
- Holweger, H. 2001, Joint SOHO/ACE workshop “Solar and Galactic Composition”, 598, 23
- Jenkins, E. B., & Shaya, E. J. 1979, *ApJ*, 231, 55
- Jenkins, E. B., & Tripp, T. M. 2001, *ApJS*, 137, 297
- Jensen, A. G., Rachford, B. L., & Snow, T. P. 2007, *ApJ*, 654, 955
- Knauth, D. C., Federman, S. R., Pan, K., Yan, M., & Lambert, D. L. 2001, *ApJS*, 135, 201
- Kopp, M., Roueff, E., & Pineau des Forêts, G. 2000, *MNRAS*, 315, 37
- McCandliss, S. R., France, K., Osterman, S., Green, J. C., McPhate, J. B., & Wilkinson, E. 2009, arXiv:0909.3878
- Meyer, D. M., Lauroesch, J. T., Sofia, U. J., Draine, B. T., & Bertoldi, F. 2001, *ApJ*, 553, L59
- Morton, D. C. 2003, *ApJS*, 149, 205
- Nehmé, C., Gry, C., Boulanger, F., Le Bourlot, J., Pineau Des Forêts, G., & Falgarone, E. 2008, *A&A*, 483, 471
- Nehmé, C., Le Bourlot, J., Boulanger, F., Pineau Des Forêts, G., & Gry, C. 2008, *A&A*, 483, 485
- Rachford, B. L., et al. 2002, *ApJ*, 577, 221
- Rachford, B. L., et al. 2009, *ApJS*, 180, 125
- Röllig, M., et al. 2007, *A&A*, 467, 187
- Savage, B. D., Bohlin, R. C., Drake, J. F., & Budich, W. 1977, *ApJ*, 216, 291
- Sembach, K. R., Savage, B. D., & Tripp, T. M. 1997, *ApJ*, 480, 216
- Sheffer, Y., Rogers, M., Federman, S. R., Abel, N. P., Gredel, R., Lambert, D. L., & Shaw, G. 2008, *ApJ*, 687, 1075
- Shull, J. M., et al. 2000, *ApJ*, 538, L73
- Shull, J. M., et al. 2009, in preparation
- Snow, T. P., & McCall, B. J. 2006, *ARA&A*, 44, 367
- Snow, T. P., Destree, J. D., & Welty, D. E. 2008, *ApJ*, 679, 512
- Sofia, U. J., Lauroesch, J. T., Meyer, D. M., & Cartledge, S. I. B. 2004, *ApJ*, 605, 272
- Sofia, U. J., & Parvathi, S. V. S. 2008, In: *Cosmic Dust - Near and Far* (Eds: T. Henning, E. Grün, J. Steinacker (San Francisco: Astr. Soc. Pacific), in press.
- Sonnentrucker, P., Friedman, S. D., Welty, D. E., York, D. G., & Snow, T. P. 2002, *ApJ*, 576, 241
- Sonnentrucker, P., Friedman, S. D., Welty, D. E., York, D. G., & Snow, T. P. 2003, *ApJ*, 596, 350
- Spitzer, L., Jr., & Jenkins, E. B. 1975, *ARA&A*, 13, 133
- Valencic, L. A., Clayton, G. C., & Gordon, K. D. 2004, *ApJ*, 616, 912
- van Dishoeck, E. F., & Black, J. H. 1988, *ApJ*, 334, 771
- Visser, R., van Dishoeck, E. F., & Black, J. H. 2009, *A&A*, 503, 323
- Wolfire, M. G., Tielens, A. G. G. M., Hollenbach, D., & Kaufman, M. J. 2008, *ApJ*, 680, 384

**Table 1**  
Stellar Parameters, Extinctions, and Hydrogen Column Densities

| Star Name    | Sp. Type           | E(B-V) | $A_V$ | ref | Log N (HI) | ref | Log N (H2) | $T_{01}$ | ref | $f^N$     |
|--------------|--------------------|--------|-------|-----|------------|-----|------------|----------|-----|-----------|
| CPD -59 2603 | O7 V               | 0.46   | ...   | 1   | 21.46      | 1   | 20.16±0.10 | 77± 11   | 8   | 0.09±0.02 |
| HD 15137     | O9.5 V             | 0.31   | ...   | 1   | 21.11      | 1   | 20.32±0.09 | 104± 21  | 9   | 0.24±0.05 |
| HD 24534     | B0 Ve              | 0.59   | ...   | 1   | 20.73      | 1   | 20.92±0.04 | 57± 4    | 6   | 0.76±0.07 |
| HD 27778     | B3 V               | 0.35   | 0.91  | 2   | 20.90      | 7   | 20.79±0.06 | 55± 7    | 6   | 0.61±0.08 |
| HD 37903     | B1.5 V             | 0.35   | 1.31  | 2   | 21.17      | 1   | 20.92±0.06 | 68± 7    | 11  | 0.53±0.07 |
| HD 40893     | B1 IV              | 0.47   | 1.32  | 2   | 21.50      | 5   | 20.58±0.05 | 78± 8    | 11  | 0.19±0.02 |
| HD 69106     | B0.5 II            | 0.20   | 0.61  | 2   | 21.08      | 1   | 19.73±0.10 | 80± 16   | 10  | 0.08±0.02 |
| HD 91824     | O6 V               | 0.24   | 0.80  | 2   | 21.15      | 3   | 20.00±0.10 | 61± 7    | 8   | 0.12±0.03 |
| HD 93205     | O3 V               | 0.38   | 1.23  | 2   | 21.33      | 1   | 19.86±0.10 | 105± 21  | 8   | 0.06±0.01 |
| HD 93222     | O8 V               | 0.36   | 1.71  | 2   | 21.54      | 3   | 19.81±0.10 | 77± 11   | 8   | 0.04±0.01 |
| HD 93843     | O6 III             | 0.27   | 1.05  | 2   | 21.33      | 1   | 19.61±0.10 | 107± 21  | 10  | 0.04±0.01 |
| HD 99857     | B0.5 Ib            | 0.33   | ...   | 1   | 21.31      | 1   | 20.25±0.10 | 83± 17   | 10  | 0.15±0.03 |
| HD 102065    | B9 IV <sup>†</sup> | 0.17   | 0.67  | 13  | 20.49      | 7   | 20.53±0.10 | 59± 7    | 12  | 0.69±0.16 |
| HD 103779    | B0.5 II            | 0.21   | 0.69  | 2   | 21.16      | 1   | 19.94±0.10 | 86± 14   | 8   | 0.11±0.02 |
| HD 104705    | B0 III             | 0.23   | 0.65  | 2   | 21.11      | 1   | 20.00±0.10 | 92± 16   | 8   | 0.13±0.03 |
| HD 115071    | B0.5 V             | 0.49   | ...   | 1   | 21.38      | 1   | 20.69±0.09 | 71± 14   | 9   | 0.29±0.06 |
| HD 116852    | O9 III             | 0.21   | 0.51  | 2   | 20.96      | 1   | 19.86±0.10 | 70± 9    | 8   | 0.14±0.03 |
| HD 121968    | B1 V               | 0.07   | ...   | 1   | 20.71      | 1   | 18.73±0.10 | 38± 3    | 8   | 0.02±0.00 |
| HD 124314    | O6 V               | 0.53   | ...   | 1   | 21.34      | 1   | 20.52±0.09 | 74± 15   | 9   | 0.23±0.05 |
| HD 147888    | B4 V               | 0.51   | 1.99  | 2   | 21.34      | 7   | 20.58±0.09 | 44± 9    | 9   | 0.26±0.05 |
| HD 152590    | O7.5 V             | 0.38   | ...   | 4   | 21.37      | 4   | 20.51±0.09 | 64± 13   | 9   | 0.22±0.04 |
| HD 157857    | O7 V               | 0.43   | 1.48  | 2   | 21.30      | 1   | 20.69±0.09 | 86± 17   | 9   | 0.33±0.07 |
| HD 177989    | B2 II              | 0.23   | 0.65  | 2   | 20.95      | 1   | 20.24±0.10 | 52± 5    | 8   | 0.28±0.06 |
| HD 185418    | B0.5 V             | 0.50   | 1.27  | 2   | 21.11      | 3   | 20.80±0.10 | 105± 21  | 8   | 0.49±0.11 |
| HD 192639    | O8 V               | 0.61   | 1.91  | 2   | 21.32      | 1   | 20.75±0.09 | 98± 15   | 9   | 0.35±0.07 |
| HD 201345    | O9 V               | 0.18   | ...   | 1   | 20.88      | 1   | 19.46±0.10 | 147± 41  | 8   | 0.07±0.02 |
| HD 203374    | B0 IV              | 0.22   | ...   | 1   | 21.11      | 1   | 20.68±0.10 | 87± 17   | 10  | 0.43±0.10 |
| HD 203532    | B5 V               | 0.28   | 0.94  | 2   | 20.78      | 7   | 20.71±0.10 | 49± 5    | 8   | 0.63±0.15 |
| HD 206267    | O6 V               | 0.52   | 1.47  | 2   | 21.30      | 6   | 20.86±0.04 | 65± 5    | 6   | 0.42±0.04 |
| HD 207198    | O9 II              | 0.54   | 1.50  | 2   | 21.34      | 1   | 20.83±0.04 | 66± 5    | 6   | 0.38±0.04 |
| HD 210839    | O6 Iab             | 0.57   | 1.15  | 2   | 21.15      | 1   | 20.84±0.04 | 72± 6    | 6   | 0.49±0.05 |
| HD 218915    | O9.5 Iab           | 0.29   | ...   | 1   | 21.11      | 1   | 20.16±0.10 | 86± 14   | 8   | 0.18±0.04 |
| HD 224151    | B0.5 II            | 0.44   | ...   | 1   | 21.32      | 1   | 20.57±0.10 | 252± 50  | 10  | 0.26±0.06 |
| HD 303308    | O3 V               | 0.45   | 1.36  | 2   | 21.45      | 1   | 20.36±0.10 | 86± 14   | 8   | 0.14±0.03 |

**References.** — (1) Diplas & Savage (1994), (2) Valencic et al. (2004), (3) Fitzpatrick & Massa (1990), (4) Cartledge et al. (2004), (5) Jensen et al. (2007), (6) Rachford et al. (2002), (7) This paper;  $N(\text{H I}) = 5.8 \times 10^{21} E(B - V) - 2N(\text{H}_2)$  as per Bohlin et al. (1978), (8) Burgh et al. (2007), (9) Sheffer et al. (2008), (10) Shull et al. (2009), (11) Rachford et al. (2009), (12) Gry et al. (2002), (13) Nehmé et al. (2008)

<sup>†</sup> See text for a discussion of the spectral type of HD 102065



**Table 2**  
Carbon Column Densities

| Star Name    | Log N (CO)   | ref | Log N (C I) <sup>†</sup> | CO/C I | err  |
|--------------|--------------|-----|--------------------------|--------|------|
| CPD -59 2603 | 14.15 ± 0.10 | 1   | 14.65                    | 0.32   | 0.08 |
| HD 15137     | 13.52 ± 0.09 | 3   | 14.60                    | 0.08   | 0.02 |
| HD 24534     | 16.13 ± 0.20 | 1   | 14.98                    | 14.08  | 7.25 |
| HD 27778     | 16.05 ± 0.14 | 1   | 15.06                    | 9.79   | 3.35 |
| HD 37903     | <13.70       | 2   | 14.22                    | <0.30  |      |
| HD 40893     | 14.18 ± 0.20 | 2   | 14.65                    | 0.34   | 0.16 |
| HD 69106     | <13.50       | 2   | 14.27                    | <0.17  |      |
| HD 91824     | <13.60       | 1   | 14.47                    | <0.14  |      |
| HD 93205     | 13.23 ± 0.06 | 1   | 14.54                    | 0.05   | 0.01 |
| HD 93222     | 13.36 ± 0.20 | 1   | 14.36                    | 0.10   | 0.05 |
| HD 93843     | <12.70       | 2   | 14.13                    | <0.04  |      |
| HD 99857     | 13.73 ± 0.10 | 2   | 14.59                    | 0.14   | 0.04 |
| HD 102065    | 13.62 ± 0.12 | 1   | 14.24                    | 0.24   | 0.07 |
| HD 103779    | <12.35       | 1   | 14.21                    | <0.01  |      |
| HD 104705    | 12.98 ± 0.16 | 1   | 14.24                    | 0.05   | 0.02 |
| HD 115071    | 14.53 ± 0.09 | 3   | 14.69                    | 0.69   | 0.16 |
| HD 116852    | 13.28 ± 0.04 | 1   | 14.15                    | 0.13   | 0.02 |
| HD 121968    | <12.30       | 1   | 13.36                    | <0.09  |      |
| HD 124314    | 14.20 ± 0.09 | 3   | 14.67                    | 0.34   | 0.08 |
| HD 147888    | 15.28 ± 0.09 | 3   | 14.70                    | 3.80   | 1.17 |
| HD 152590    | 13.77 ± 0.09 | 3   | 14.60                    | 0.15   | 0.03 |
| HD 157857    | 14.08 ± 0.09 | 3   | 14.62                    | 0.29   | 0.07 |
| HD 177989    | 14.62 ± 0.17 | 1   | 14.68                    | 0.87   | 0.35 |
| HD 185418    | 14.82 ± 0.20 | 1   | 14.74                    | 1.20   | 0.57 |
| HD 192639    | 13.78 ± 0.09 | 3   | 14.73                    | 0.11   | 0.03 |
| HD 201345    | <12.40       | 1   | 13.93                    | <0.03  |      |
| HD 203374    | 15.35 ± 0.10 | 2   | 14.98                    | 2.34   | 0.60 |
| HD 203532    | 15.70 ± 0.17 | 1   | 14.75                    | 8.95   | 4.07 |
| HD 206267    | 16.11 ± 0.13 | 1   | 15.32                    | 6.10   | 1.96 |
| HD 207198    | 15.53 ± 0.20 | 1   | 15.26                    | 1.88   | 0.89 |
| HD 210839    | 15.41 ± 0.08 | 1   | 15.00                    | 2.59   | 0.56 |
| HD 218915    | 13.64 ± 0.13 | 1   | 14.54                    | 0.13   | 0.04 |
| HD 224151    | 13.85 ± 0.06 | 2   | 14.63                    | 0.17   | 0.03 |
| HD 303308    | 13.65 ± 0.06 | 1   | 14.73                    | 0.08   | 0.02 |

**References.** — (1) Burgh et al. (2007), (2) This paper, (3) Sheffer et al. (2008)

<sup>†</sup> Errors for C I are assumed to be 0.05 dex in all cases except for HD 24534, HD 147888, and HD 203534, which are assigned an error of 0.10 dex. See text for discussion.